

Shoreline Change with Groin Coastal Protection Structure at North Java Beach

Oki Setyandito^{1*}, Aldo Christanto Purnama², Nur Yuwono³,
Juliastuti⁴, and Yureana Wijayanti⁵

^{1,2,4,5}Civil Engineering Department, Faculty of Engineering, Bina Nusantara University
Jln. K.H. Syahdan No. 9, Jakarta Barat 11480, Indonesia

³Department of Civil and Environmental Engineering, Faculty of Engineering, Gadjah Mada University
Jln. Grafika No. 2, Daerah Istimewa Yogyakarta 55281, Indonesia

¹osetyandito@binus.edu; ²aldo.purnama@binus.edu; ³nuryuwono@ugm.ac.id;
⁴yuliastuti@binus.edu; ⁵yureana.wijayanti@binus.ac.id

Received: 24th September 2019/ Revised: 21st January 2020/ Accepted: 28th January 2020

How to Cite: Setyandito, O., Purnama, A. C., Yuwono, N., Juliastuti, & Wijayanti, Y. (2020). Shoreline Change with Groin Coastal Protection Structure at North Java Beach. *ComTech: Computer, Mathematics and Engineering Applications*, 11(1), 19-28. <https://doi.org/10.21512/comtech.v11i1.6022>

Abstract - The research aimed to study the effect of groin application to erosion at the shoreline. The method utilized the bathymetry and topography data of north beach of Balongan, West Java. Modeling of the shoreline change due to groin installment used software called GENESIS. Based on analysis result, it is found that the significant wave direction comes from the southeast with significant wave height of 1,18 meters and surf zone width of 140 meters. It is concluded that at research area of north beach of west Java, I-groin with length of 70 meters and T head groin of 60 meters in long T-groin effectively overcome erosion and advance the coastline by 10786,62 m² or in average 6,3 meters.

Keywords: shoreline change, groin coastal protection structure

I. INTRODUCTION

Climate change affects the coastal environment. Coastal erosion is one of the climate change effects on the coastal areas (Martins, De Souza Pereira, Silva-Casarin, & Neto, 2017). Coastline along the north and south of Java in Indonesia are densely populated and prone to beach erosion (Setyandito, Nizam, Yuwono, & Triatmadja, 2012a; Setyandito, Nizam, Triatmaja & Yuwono, 2012b; Setyandito, Yuwono, Triatmodjo, Bakti, & Kesuma, 2014). There should be a protection structure to prevent or reduce these erosional processes (Mohanty *et al.*, 2012). Groins are beach protection structure against erosion. It is narrow structures with variable lengths and heights and usually constructed

perpendicular to the shoreline (Sadeghi & Dania, 2019). Groins can be built as a single structure or in series as a groin field (Neshaei & Biria, 2013; Tereszkievicz, McKinney, & Meyer-Arendt, 2018). Next, Balas, Inan, and Yilmaz (2011) and Oyedotun (2014) analyzed three groin series on shoreline change and proposed numerical model ((GENERalized model for SIMulating Shoreline change (GENESIS)). They concluded that this model agreed with the physical model. Similarly, Alireza, Hamed, Ali, and Hamid (2016) and Fatimah, Ariff, and Aulia (2015) carried a physical model and concluded that groin spacing should be equal to groin length. Moreover, Mohanty *et al.* (2012) investigated the effects of groins on shoreline changes by using a three-dimensional physical model. Then, Rocha, Coelho, and Fortes (2013) and Noujas and Kankara (2018) proposed a numerical model to calculate the shoreline changes in placing groin. They used only longshore sediment transport and compared their model with field data.

Similarly, Sume (2018) and Thomas and Dwarakish (2015) suggested a numerical model simulate the short-term temporal changes in shoreline position due to structure interrupting the longshore sediment transport. Moreover, Süme (2014), Sume (2018), McCarroll *et al.* (2018), and Török, Baranya, Rütther, and Spiller (2014) studied the effects of T-groin and straight groin parameters on the accretion in a physical model in a three-dimensional wave basin. They used regular waves and analyzed the effect of groin parameters on accretion value. Then, Setyandito, Nizam, Yuwono, and Triatmaja (2011) studied the effect of shoreline stability between I- and L-groin using a three-dimensional physical model. They suggested that

the distance of headland (B) of L-groin and length of the detached breakwater (L) affected the formation of tombolo or salient. They suggested tombolo formation started when it is $B/L > 1,1$. Besides, Hutahaean (2018) proposed a stable shoreline equation between two groins (T and I) based on the assumption that net shoreline change before and after the construction of groin was zero. Meanwhile, Niculescu and Rusu (2018) proposed a way to use Log-Spiral equation for stable shoreline submitted by Claudino-Sales, Wang, and Carvalho (2018), Parabolic Bay Shape equation by El-Shinnawy, Medina, and González (2017), and Tangent Hyperbolic Bay Shape by Kemp, Vandeputte, Eccleshall, Simons, and Troch (2018). Then, Silveira, Klein, and Tessler (2010) proposed that the Parabolic Bay shape could be used to predict stable shoreline equations caused by the headland of the groin.

Sola, Kavianpour, and Tabatabai (2015) examined the hydraulics of sediment transport behavior with various groin spacing. Then, Di Bona (2013), Ayyappan and Thiruvengkatasamy (2018), Mohanty *et al.* (2012), and Setyandito *et al.* (2012a) studied the effect of groin structures on stable beaches. They also analyzed groin parameters affecting the shoreline changes using a three-dimensional physical model. The researchers further continue the research on the effect of groin application to erosion at the shoreline. The aim of the research is to analyze effective groin design, simulate wave variation influence to groin type to yield empirical equation.

II. METHODS

The research utilizes Nearshore Evolution Modeling System (NEMOS), numerical model to get the result of shoreline change with various groins. It is by a the data from survey and secondary data such as previous research and available data from national services. Bathymetry and topography data used in the research are done by direct surveying on site. Topography data are gathered using theodolite and water pass leveling. Meanwhile, bathymetry data are collected from the partnership with Water Resources Laboratory at Gajah Mada University. The data are gathered around 4.200 meters across the shoreline and 800 meters seaward from the shore. It can be seen in Figure 1. Data regarding wind are obtained from the National Oceanic and Atmospheric Administration (NOAA), which is recorded every three hours. Then, the recorded data are converted to wave data (hindcasting) using the Simplified Method for Estimating Wave Condition (SMB) method by Shore Protection Manual. The wind speed is converted to wave height and period using Equation (1) and (2). In addition, secondary data such as nationally available wind data and sediment data from previous research are utilized in the research (Coastal Engineering Research Center (US), 1984).

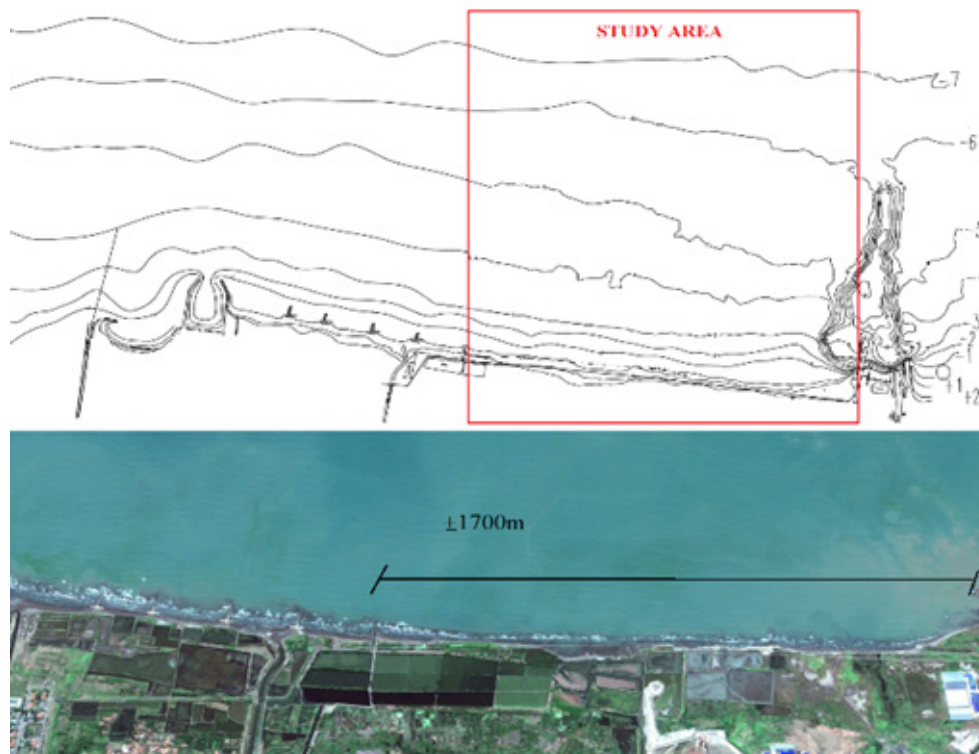


Figure 1 Bathymetrical and Topography Data
(The Red Box is an Area of GENESIS Model in This Research)

$$H_s = \frac{0,0016 \left(\frac{gF}{U_a^2} \right)^{\frac{1}{2}} U_a}{g} \quad (1)$$

$$T_p = \frac{0,2857 \left(\frac{gF}{U_a^2} \right)^{\frac{1}{3}} U_a}{g} \quad (2)$$

Where:

H_s : Significant wave (m);

T_p : Wave Period (s);

g : Gravity (m/s²);

F : Fetch (m);

U_a : Wind speed (m/s);

t : Wind duration (hour).

Further analysis using Coastal Engineering Design and Analysis System (CEDAS) software concludes the Waverose as seen in Figure 2. It can be stated that the dominant wave comes from the southeast with a significant wave height of 1,18 meters and a period of 5,12 seconds. Sediment data needed for modeling are D50 or median diameter of soil data in site location. The data used are from previous research done by the Bandung Institute of Technology (Muin, Idris, & Yuanita, 2016). Modeling is done with GENESIS presenting in NEMOS set of codes within CEDAS. GENESIS allows simulation of shoreline change due to wave action occurring from the period of a month to years (Hanson, 1989; Oyedotun, 2014). Proposed by Hanson (1989) and Kemp *et al.* (2018), data needed for modeling are a periodical wave, bathymetrical, and topography data as an input with a simulation period of 10 years or 120 months used in this research.

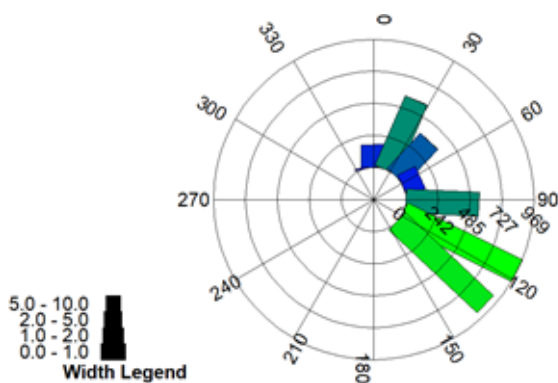


Figure 2 Waverose

Then, the model is calibrated using two different shorelines (2010 and 2019) to get the values of K_1 and K_2 . It controls the amount of sediment transported due

to wave action in the reigning conservation of mass equation, as seen in Equation 3. Sediment transported is controlled by Equation 4. Then, a_1 and a_2 are empirical equations controlled by K_1 and K_2 (Equation (5) and (6)) (Di Bona, 2013).

$$\frac{\partial y}{\partial t} = \frac{(\delta Q + q)}{D_B + D_C} = 0 \quad (3)$$

$$Q = \left(H^2 C_{\underline{g}} \right)_b \left(a_1 \sin 2\theta_{bs} - a_2 \cos 2\theta_{bs} \frac{\partial H}{\partial x} \right)_b \quad (4)$$

$$a_1 = \frac{K_1}{16(S-1)(1-p)(1,416)^3} \quad (5)$$

$$a_2 = \frac{K_2}{8(S-1)(1-p)\tan\beta(1,416)^2} \quad (6)$$

Where:

K_1 and K_2 : Coefficient

S : ρ_s / ρ

ρ_s : Sand density (assumed $2,65 \cdot 10^3$ kg/m³)

p : Sand porosity (assumed = 0,4)

$\tan \beta$: Beach slope

1,416: Wave height conversion H_{m0}

a_1 : Empirical equation controlled by K_1

a_2 : Empirical equation controlled by K_2

The calibration result can be observed in Figure 3. The red line is the reference shoreline (2019), and the black line is the initial shoreline position (2010). In this particular beach, the K_1 is 0,25, and K_2 is 0,13. These values are used in further modeling. Modeling of shoreline change using CEDAS can be categorized into three parts. There are domain making, wave data analysis, and GENESIS. Domain making is done by the input of the bathymetrical data and topographical data from the survey in xyz format.

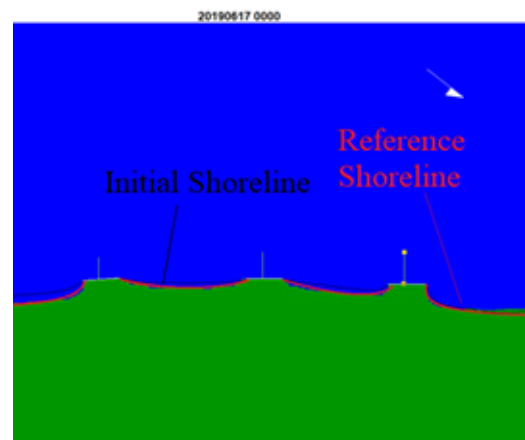


Figure 3 Calibration Result

It is done using GridGen code inside CEDAS. After inputting our input data, the selection of domain is then done and exported for input in GENESIS. Wave data analysis is done by inputting original periodical data to Wave, Winds, and Water Levels (WWWL) code. Then, the result from WWWL is inputted to WSAV to get a permutation wave file. It is used for inputting data for SpecGen. Next, wave spectrum output from SpecGen is used for input for Steady State Spectral Wave (STWAVE) for updated breaking wave station for running GENESIS.

GENESIS is run by the input data from wave analysis and domain making. Then, boundary conditions are specified, such as D_{50} , K_1 , and K_2 , and the existing or designed coastal structures can be defined in this code. After all input data are fulfilled, the model can be run to get shoreline changes with specified simulation time. The graphical flowchart of NEMOS within CEDAS can be seen in Figure 4.

III. RESULTS AND DISCUSSION

The first run model is the 10-year simulation with no coastal protection. It will give an idea of erosion happening. It is also a benchmark for analysis and the effect of the groin in addition to shoreline change.

The methodology utilized in both, this research and the preliminary one (Setyandito *et al.* 2011), has shown good performance in analyzing the groin structures influence to coastal line changes. New coastline stability process established by the

performance of the groin system has been studied using numerical modeling with the variation of wave direction for most effective groin formation (Wardani, & Murakami, 2019). Therefore, the researchers divide the results into three main categories. Those are effective groin design, wave variation (amplification factor as boundary input for GENESIS), and analytical analysis to yield empirical equation. The result of the model for ten years without protection structure can be observed in Figure 5. It is shown in the x- and y-axis, which can be seen in Figure 6. There are two points where major erosion occurs when 10-year simulations are run (Figure 5). The difference between the two lines is calculated to get the areal shoreline change (m^2). Then, it is divided by the modeled length, which is 1700 m to get shoreline change in meters. If the initial shoreline is in front of the simulation result, it can be said that erosion will likely occur in that area. If the simulation result is in front of the initial shoreline, that area is predicted for accretion to occur.

Effective groin design is obtained by variation of spacing, length, and space of groin. It is to decide the parameter of the shoreline change in meters. After the calculation of wave data is obtained, the data analysis is as follows:

- Significant wave height = 1,18 meters
- Significant wave period = 5,12 seconds
- Beach slope (m/m) = 0,01
- Breaking wave height = 1,15 meters
- Breaking wave depth = 1,42 meters
- Surf zone width = 140 meters

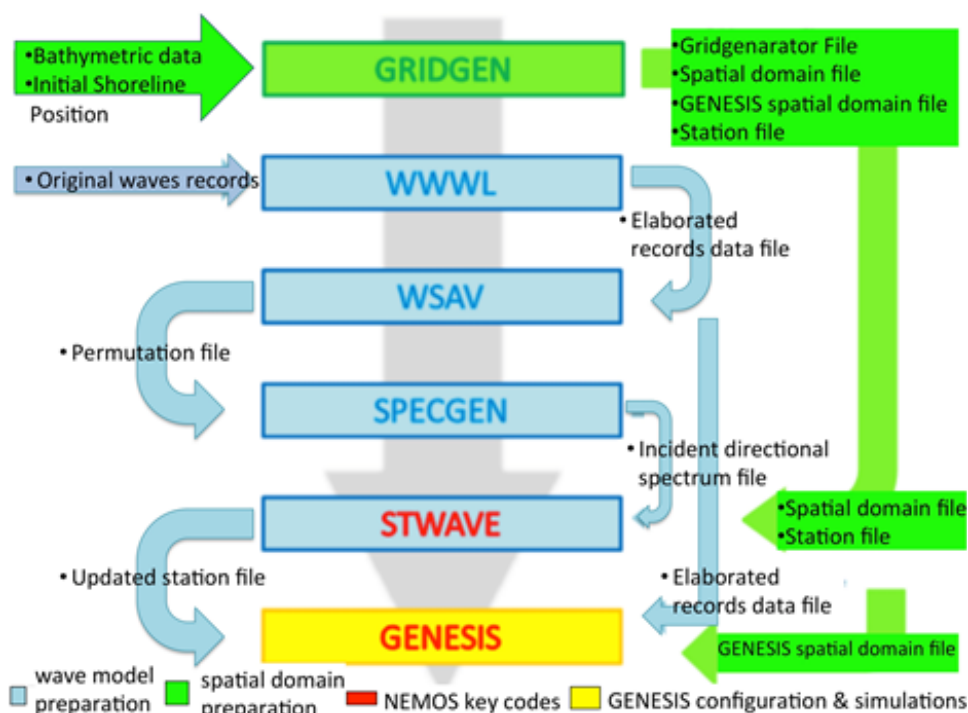


Figure 4 Flowchart of NEMOS within CEDAS

When the result of wave data calculation is achieved, the modeling of variation of groin spacing is done. It is with the length of groin 50% of surf zone width (70 meters) and spacing of 1-3 times (70, 140, and 210 meters) and the length of the groin, according to Van der Meer (2017).

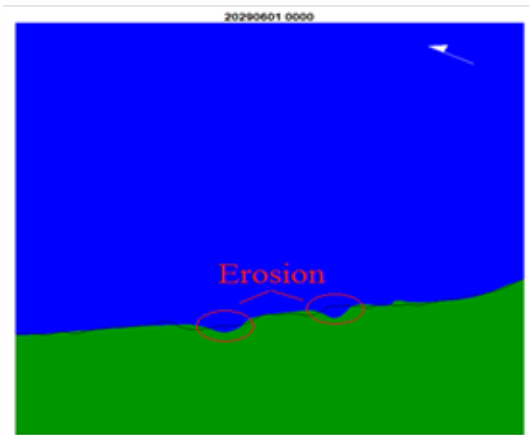


Figure 5 The Result of 10-Year Simulation without Protection Structure

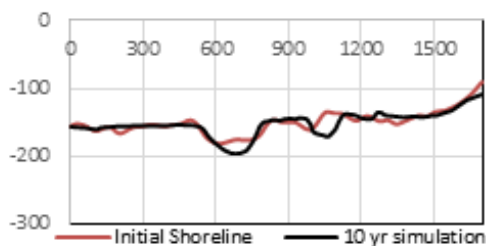


Figure 6 The Result of 10-Year Simulation without Protection Structure (X and Y)

Next, the variation of groin length and shape (T-groin) is placed where erosion still occurs in the 140 meters variation with the variation of length of 40-60% of the surf zone (Van der Meer, 2017). Then, from these variations, there is evidence of effective groin variation to overcome erosion problems. Data on shoreline change can be observed in Table 1. The running result is in Figure 7. From these data, it can be concluded that the effective groin is a combination of T (70 m) and I (60 m) groin with a spacing of 140 meters.

Wave variation is done to get different wave steepness by modifying the boundary input of GENESIS (wave height amplification factor) to get different wave steepness (Hs/L). Amplification factor used in this research is 0,6; 0,8; 1, 1,2; and 1,5. The 0,6 represents calm wave, and 1,5 shows storm wave. The variation of amplification to wave steepness data can be seen in Table 2.

Then, the result from groin spacing and length variation is run with different wave amplification factor. It is done to get the effect of different wave action to shoreline change with groin characteristics. Data obtained from the running model can be seen in Table 3 for groin spacing and Table 4 for groin length variation.

Table 1 Variation of Groin Length and Shape, and Shoreline Change

Variation	Area of Shoreline Change (m ²)	Length of Shoreline Change (m)
Without Groin	-1428,76	-0,840
Groin Spacing 70m	302,15	0,177
Groin Spacing 140m	7222,23	4,248
Groin Spacing 210m	-1062,43	-0,625
T-Groin Length 70m	8342,58	4,849
T-Groin Length 60m	10786,62	6,345
T-Groin Length 85m	7669,41	4,511

Shoreline change parameter (P) is divided by groin parameters such as groin spacing (S) and groin length (Lg) to give non-dimensional parameters (P/S and P/Lg) to be plotted against wave steepness (Hs/L) for further analysis. The analytical study related to wave action to sedimentation due to the groin parameter can be seen in Table 4. Then, wave steepness is put in the x-axis, and P/S and P/Lg are in the y-axis in two different graphs (Figure 8 and Figure 9).

Table 2 Non-dimensional parameter P/S

Amplification Factor	Areal Shoreline Change (m ²)	Shoreline Change P(m)	Groin Spacing S(m)	P/S
0,6	439,84	0,26	70	0,0037
	7236,41	4,26	140	0,0304
	966,61	0,57	210	0,0027
0,8	369,56	0,22	70	0,0031
	7322,37	4,31	140	0,0308
	963,22	0,57	210	0,0027
1	302,15	0,18	70	0,0025
	7222,22	4,25	140	0,0303
	-1062,48	-0,63	210	-0,0030
1,2	209,71	0,12	70	0,0018
	6892,12	4,05	140	0,0290
	-2369,74	-1,39	210	-0,0066
1,5	709,61	0,42	70	0,0060
	6367,91	3,75	140	0,0268
	-2776,91	-1,63	210	-0,0078

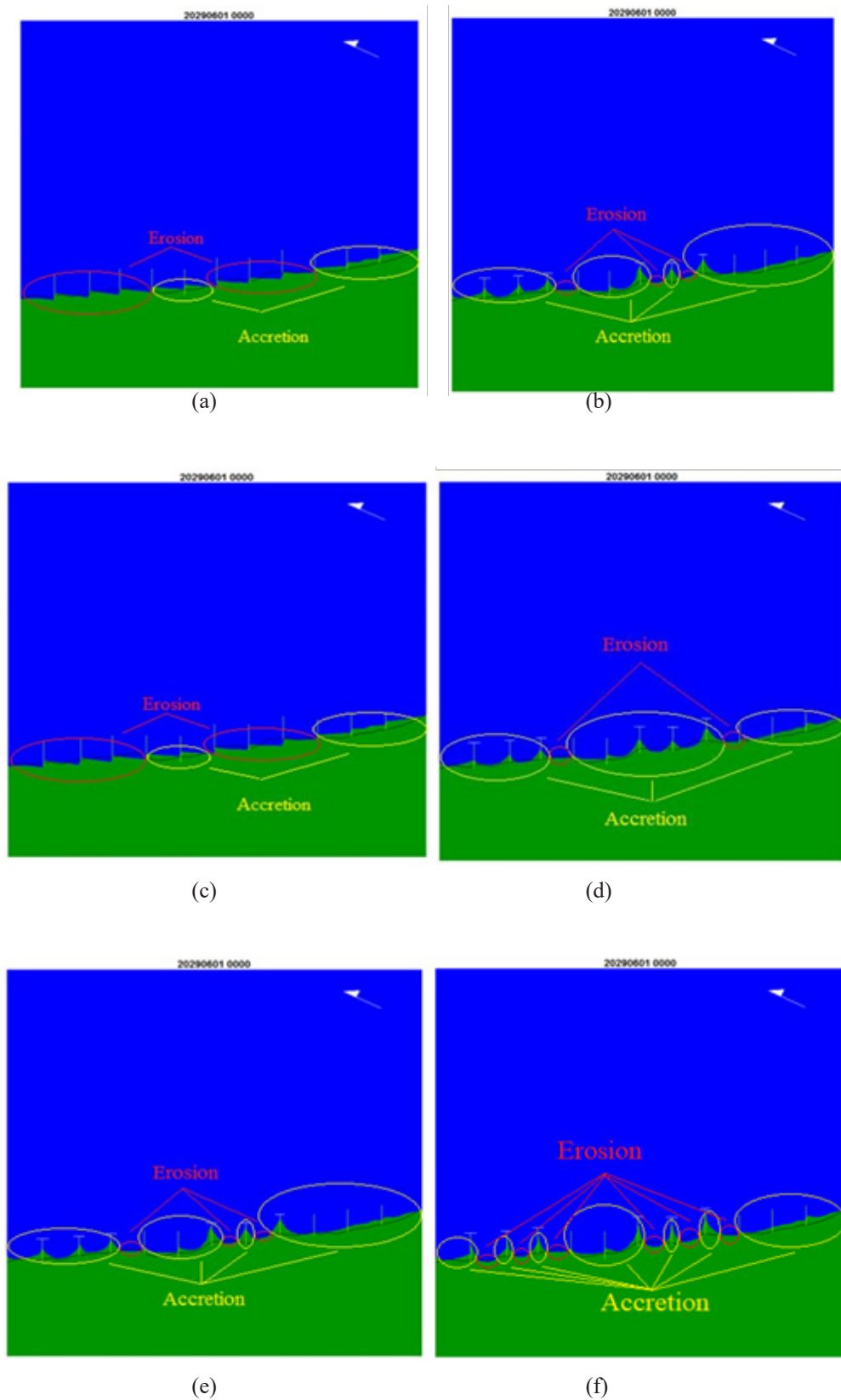


Figure 7. Running Result (a) Spacing of 70 meters, (b) Spacing of 140 meters, (c) Spacing of 210 meters, (d) T-Groin (60m) and I-Groin (70m) Spacing 140 meters (e) T-Groin (70m) and I-Groin (70m) Spacing 140 meters, (f) T-Groin (85m) and I-Groin (70m) with Spacing of 140 meters

Table 3 Non-dimensional parameter P/Lg

Amplification Factor	Areal Shoreline Change (m ²)	Shoreline Change P (m)	Groin Length Lg (m)	P/Lg
0,6	13368,36	7,86	60	0,1311
	9513,00	5,60	70	0,0799
	7899,74	4,65	85	0,0547
0,8	10169,63	5,98	60	0,0997
	8944,58	5,26	70	0,0752
	7474,00	4,34	85	0,0517
1	10786,62	6,35	60	0,1058
	8342,58	4,91	70	0,0701
	7669,41	4,51	85	0,0531
1,2	10093,64	5,94	60	0,0990
	8339,79	4,91	70	0,0701
	6879,36	4,05	85	0,0476
1,5	9561,26	5,62	60	0,0937
	7666,49	4,51	70	0,0644
	6795,20	3,99	85	0,0470

Table 4 Wave steepness against P/S and P/Lg

Amplification Factor	Wave Steepness (Hs/L)	P/S	P/Lg
0,6	0,0182	0,0037	0,1311
	0,0182	0,0304	0,0799
	0,0182	0,0027	0,0547
0,8	0,0242	0,0031	0,0997
	0,0242	0,0308	0,0752
	0,0242	0,0027	0,0517
1	0,0303	0,0025	0,1058
	0,0303	0,0303	0,0701
	0,0303	-0,0030	0,0531
1,2	0,0363	0,0018	0,0990
	0,0363	0,0290	0,0701
	0,0363	-0,0066	0,0476
1,5	0,0454	0,0060	0,0937
	0,0454	0,0268	0,0644
	0,0454	-0,0078	0,0470

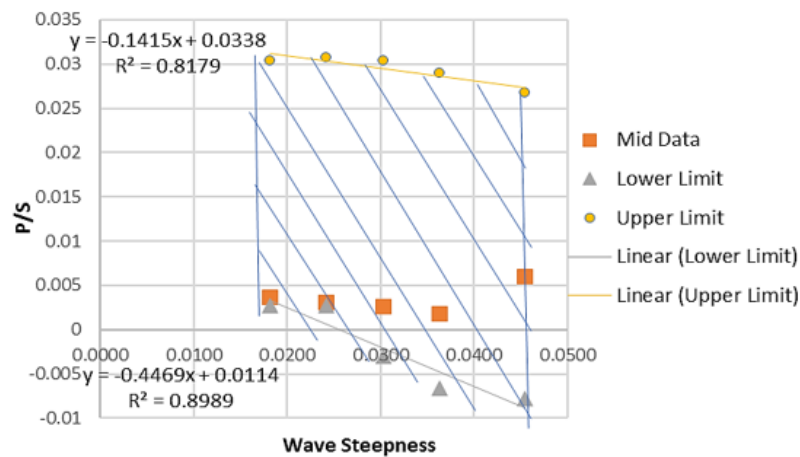


Figure 8 Upper and Lower Limit of Wave Steepness with P/S

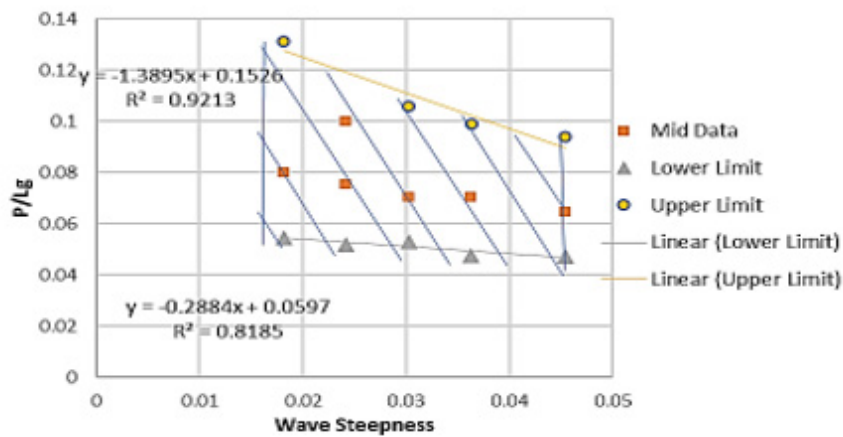


Figure 9 Upper and Lower Limit of Wave Steepness with P/Lg

These two equations are used to represent the area of parameter $y = mx + c$ with m and c values ranging from the lower and upper limits. From the graph in Figure 8, upper limit line and lower limit line equations are $y = -0,1415x + 0,0338$ and $y = -0,4469x + 0,0114$. Both equations represent the blue shaded area. Then, the linear equation of $y = (a_1)x + a_2$ is developed based on the upper and lower equations. Finally, the relationship equation between wave steepness and coastline change regarding the distance between groin is $y = (-0,1415 \sim -0,4469)x + (0,0114 \sim 0,0338)$, and substitute x with $\frac{2\pi H_s}{gT^2}$ and y with $\frac{P}{S}$, so the empirical equation is:

$$\frac{P}{S} = (a_1)\left(\frac{2\pi H_s}{gT^2}\right) + (a_2) \quad (7)$$

Where:

- P : Coastline change (m)
- S : Distance between two groins (m)
- a_1 : Empirical coefficient 1 with distance (-0,1415 ~ -0,4469)
- a_2 : Empirical coefficient 2 with distance (-0,0114 ~ -0,0338)
- H_s : Significant wave height (m)
- T : Wave period (m)
- g : Gravity (9,81 m/s²)

Figure 9 shows the analysis graph of the result about the relationship between coastline change (P), groin length (Lg), and wave characteristics ($\frac{H_s}{L}$). The

upper limit line and lower limit line equations are $y = -0,3895x + 0,1526$ and $y = -0,2884x + 0,0597$. Then, the linear equation of shaded area is $y = (-0,2884 \sim -1,3895)x + (0,0597 \sim 0,1526)$. Then, with the substitute of the wave steepness, x with $\frac{2\pi H_s}{gT^2}$, sedimentation

characteristics influenced by groin length, and y with P/Lg , the empirical equation is:

$$\frac{P}{Lg} = (a_3)\left(\frac{2\pi H_s}{gT^2}\right) + (a_4) \quad (8)$$

Where:

- P : Coastline change (m)
- Lg : Groin length (m)
- a_3 : Empirical coefficient 3 with distance (-0,2884 ~ -1,3895)
- a_4 : Empirical coefficient 4 with distance (0,0597 ~ 0,1526)
- H_s : Significant wave height (m)
- T : Wave period (m)
- g : Gravity (9,81 m/s²)

From both Equations (7) and (8), it can be said that the steeper the slope or, the higher the H_s/gT^2 value is, the higher the possibility of erosion

occurrence will be. If the equation is $y = -mx + c$, the negative (-) sign of m shows the reverse relationship among parameters. A decrease of y -values follows the increases of x -values. This result indicates as the higher the wave steepness is, the higher the wave height is too. This phenomenon results in higher sediment transport compared to lower wave steepness. Wave energy is influenced by quadratic breaking wave height. Therefore, the increase in wave height is followed by an increase in sedimentation.

Similarly, wave energy is influenced by the quadratic of breaking wave height. So, a double increase in wave height will quadruple the wave energy. Sediment transport correlates with wave energy generated by breaking waves. Thus, it can be concluded that the higher the wave height is, the larger wave energy generated will be. It can transport a large amount of sediment and cause bigger erosion compared to lower wave height.

The calculation of coastline change due to spatial and temporal of longshore transport from the breaking wave is performed by GENESIS numerical application. The benefit of this program is that it can predict the long term trend of coastline as a response to breaking waves. The simulation period ranges from 6 to 100 months, and the gap between groin can vary from 1 to 100 km. The large wave data interval is within the range of 30 minutes and up to 6 hours. However, there are several constraints of this program that should be taken into considerations during the data analysis. GENESIS ignores sediment transport from cross-shore transport. It can only be utilized to predict coastline changes due to coastal structure and changes due to the breaking wave. However, it cannot be used to calculate the refraction of waves, estimate coastline change caused by storm events, and assess the tidal effect on the coastline.

GENESIS is utilized to predict the longshore transport on the beach, and analyze coast line change. The boundaries applied in this program are the constant shape of the beach profile, accretion, and erosion. Those will not change the beach profile. The breaking wave causes sediment transport along the beach line. The structured detail surrounding the nearshore is not taken into consideration, and beach composition is a sand beach.

The beach has a dynamic balance between adapting to its preliminary condition as a response to breaking the incoming wave energy. The normal onshore wave is easier to be broken down by beach mechanism. The storm or large wave has significant energy, although it only occurs in a short time. It can lead to erosion. After erosion takes place, there are two conditions of coastline following the erosion. The first is the sediment material. It is transported back to its previous location. The second is the sediment material. It will move to another location and will not return. This condition will cause erosion in one place and sedimentation in another location.

As a storm occurs, wave energy generated cannot be buffered by the beach's natural protection

ability. As a result, erosion occurs. After the storm event, the beach condition will gradually back to its original shape due to sediment material. It is transported back to the beach by the onshore direction currents. However, some of the materials are not transported to their original location. Storm waves can cause erosion because when the storm occurs, the significant intensity of perpendicular current to the beach carries to the beach material. In general, this erosion is caused by storm wave transpires in a short period and lasts only in a short time or temporarily. The material that is transported by the current is stored in a surf zone. It is returned to the beach as the wave is swelling or calmer. However, if the beach bathymetry is steep and falls into the sea gorges, these sediments cannot transport back to the beach.

Increase of wave steepness means more significant wave energy in a wave group. It is due to the higher wave height compared to other wave height within a wave group with a similar wavelength. It can be highlighted that the magnitude of sediment transport is influenced by breaking wave height and the energy within that wave.

IV. CONCLUSIONS

In the research, the input data range from 2010 to 2019, with wave height and wave period of 1,19 m and 5,12 seconds, respectively. Wave data from the hindcasting process are utilized in GENESIS model with ten years of simulation time. The simulation result of no protection beach shows beach erosion occurred up to the pipeline system. Groin can be used as coastal protection at North Java beach to protect the coastline area because the oblique wave angle comes to the shoreline, making the dominant sediment transport to longshore transport. Combination of I-and T-groin and spacing of 140 meters can effectively reduce erosion at the shoreline. To enhance the process of stable dynamic beach conditions and to minimize downdrift erosion effect due to groin structure, beach nourishment should be applied between the groins. The theoretical equation on the relationship between wave slope and shoreline changing due to groin structure is also developed in this research.

Further analysis is needed to validate this empirical equation. Therefore, several suggestions for future research are proposed. First, the research can utilize the physical model or onsite survey of the existing coastal structure to validate the data from the GENESIS outcome. Second, the research can use the application for different beach characteristics. Third, the research should prepare an anticipation act to prevent sediment deficit at the downdrift side due to the movement of the beach line down to the groin field.

ACKNOWLEDGEMENTS

The researchers would like to thank Pusat Studi Ilmu Teknik (PSIT), Faculty of Engineering of Gadjah Mada University, and PT Pertamina (Persero) RU-VI

Balongan, West Java for the research collaboration.

REFERENCES

- Alireza, M., Hamed, O., Ali, L. Y. M., & Hamid, H. (2016). Numerical investigation of flow around groins in barotropic condition. *International Journal of Structural and Civil Engineering Research*, 5(4), 285-291.
- Ayyappan, K., & Thiruvengatasamy, K. (2018). On the hydrodynamics of shoreline morphological changes and its impact on tidal stability in the presence of groins using field measurements at Muttukadu Estuary. *International Journal of Civil Engineering and Technology (IJCIET)*, 9(6), 912-922.
- Balas, L., Inan, A., & Yilmaz, E. (2011). Modelling of sediment transport of Akyaka Beach. *Journal of Coastal Research*, (Special Issue 64), 460-463.
- Claudino-Sales, V., Wang, P., & Carvalho, A. M. (2018). Interactions between various headlands, beaches, and dunes along the coast of Ceará state, Northeast Brazil. *Journal of Coastal Research*, 34(2), 413-428.
- Coastal Engineering Research Center (US). (1984). *Shore Protection Manual*. Department of the Army, Waterways Experiment Station, Corps of Engineers, Coastal Engineering Research Center.
- Di Bona, S. (2013). *Modeling of coastal evolution: Long term simulation in the Vagueira region* (Master Thesis). University of Padova.
- El-Shinnawy, A., Medina, R., & González, M. (2017). *Equilibrium planform of headland bay beaches: Effect of directional wave climate*. Retrieved from http://coastaldynamics2017.dk/onewebmedia/020_Elshinnawy_Ahmed.pdf
- Fatimah, E., Ariff, A., & Aulia, T. B. (2015). The influence of single zigzag type porous groin in the change of beach profile. *Procedia Engineering*, 125, 257-262.
- Hanson, H. (1989). GENESIS: A generalized shoreline change numerical model. *Journal of Coastal Research*, 5(1), 1-27.
- Hutahaean, S. (2018). Comparative study between Groin and T-Head Groin. *International Journal of Advanced Engineering Research and Science (IJAERS)*, 5(11), 1-5.
- Kemp, J., Vandeputte, B., Eccleshall, T., Simons, R., & Troch, P. (2018). A modified hyperbolic tangent equation to determine equilibrium shape of headland bay beaches. *Coastal Engineering Proceedings*, 36, 106-106.
- Martins, K. A., De Souza Pereira, P., Silva-Casarin, R., & Neto, A. V. N. (2017). The influence of climate change on coastal erosion vulnerability in northeast Brazil. *Coastal Engineering Journal*, 59(2), 1740007-1-1740007-25
- McCarroll, R. J., Masselink, G., Valiente, N. G., Scott, T., King, E. V., & Conley, D. (2018). Wave and tidal controls on embayment circulation and headland bypassing for an exposed, macrotidal site. *Journal of Marine Science and Engineering*, 6(3), 1-32.
- Mohanty, P. K., Patra, S. K., Bramha, S., Seth, B., Pradhan,

- U., Behera, B., ... & Panda, U. S. (2012). Impact of groins on beach morphology: A case study near Gopalpur Port, East Coast of India. *Journal of Coastal Research*, 28(1), 132-142.
- Muin, M., Idris, K., & Yuanita, N. (2016). Application of large-scale 3D non-orthogonal boundary fitted sediment transport model and small-scale approach for offshore structure in Cimanuk Delta North Java Sea. *Journal of Engineering and Technological Sciences*, 48(3), 301-319.
- Noujas, V., & Kankara, R. (2018). Shoreline prediction using a numerical model along rathnagiri coast, West Coast of India. In *6th National Conference on Coastal, Harbour and Ocean Engineering*.
- Neshaei, M. L., & Biria, H. A. (2013). Impact of groyne construction on beach: Case study Anzali & Astar Coasts. In *7th National Congress on Civil Engineering* (pp. 7-8).
- Niculescu, D. M., & Rusu, E. V. (2018). Evaluation of the new coastal protection scheme at Mamaia Bay in the nearshore of the Black Sea. *Ocean Systems Engineering-an International Journal*, 8(1), 1-20.
- Oyedotun, T. D. (2014). Shoreline geometry: DSAS as a tool for historical trend analysis. *Geomorphological Techniques*, 3(2.2), 1-12.
- Rocha, M. V. L., Coelho, C., & Fortes, C. J. E. M. (2013). Numerical modeling of groin impact on nearshore hydrodynamics. *Ocean engineering*, 74(December), 260-275.
- Sadeghi, K., & Dania, A. L. (2019). An introduction to onshore structures' construction. *Academic Research International*, 10(1), 1-12.
- Setyandito, O., Nizam, N., Yuwono, N., & Triatmaja, R. (2011). Performance of Groin Type-I and Type-L in maintaining shoreline stability. In *International Seminar on Water Related Risk Management*.
- Setyandito, O., Nizam, N., Yuwono, N., & Triatmadja, R. (2012a). Pengaruh gelombang pada profil kemiringan pantai pasir buatan (Uji model fisik dan studi kasus penanggulangan erosi serta pendukung konservasi lingkungan daerah pantai). *Jurnal Sains & Teknologi Lingkungan*, 4(1), 32-42.
- Setyandito, O., Nizam, N., Triatmaja, R., & Yuwono, N. (2012b2). The profile stability of the artificial sand beach nourishment. *International Journal of Civil & Environmental Engineering*, 12(02), 36-41.
- Setyandito, O., Yuwono, N., Triatmodjo, B., Bakti, T. E., & Kesuma, L. M. (2014). Stability of armour layer under wave attack, 2-D physical model and case study in South Java coastline, Indonesia. *World Applied Sciences Journal*, 32(3), 415-421.
- Silveira, L. F., Klein, A. H. D. F., & Tessler, M. G. (2010). Headland-bay beach planform stability of Santa Catarina state and of the Northern Coast of São Paulo state. *Brazilian Journal of Oceanography*, 58(2), 101-122.
- Sola, S. A., Kavianpour, M. R., & Tabatabai, M. R. M. (2015). Experimental study of scour depth in attracting groins series. In *Scientific Cooperations Workshops on Engineering Branches*.
- Süme, V. (2014). Grain size and beach formation characteristic at the T-Head Groins System at Kiyicik, Turkey (Eastern Black Sea). *Journal of Civil & Environmental Engineering*, 4(4), 1-5.
- Sume, V. (2018). Shoreline changes in three groin fields on the eastern Black Sea Coast. *Fresenius Environmental Bulletin*, 27(1), 125-131.
- Tereszkiewicz, P., McKinney, N., & Meyer-Arendt, K. J. (2018). Groins along the Northern Yucatan Coast. *Journal of Coastal Research*, 34(4), 911-919.
- Thomas, T. J., & Dwarakish, G. S. (2015). Numerical wave modelling—A review. *Aquatic Procedia*, 4, 443-448.
- Török, G. T., Baranya, S., Rüter, N., & Spiller, S. (2014). Laboratory analysis of armor layer development in a local scour around a groin. In *Proceedings of the International Conference on Fluvial Hydraulics River Flow* (pp. 3-5).
- Van der Meer, J. W. (2017). Geometrical design of coastal structures. In K. Pilarczyk (Ed.), *Dikes and revetments* (pp. 161-176).
- Wardani, K. S., & Murakami, K. (2019). The effectiveness of groin system on the control of sediment transport. *Journal of Japan Society of Civil Engineers, Ser. B2 (Coastal Engineering)*, 75(2), I_535-I_540.